

Circulation and suspended sediment transport in a sediment starving ria: the Itapessoca

José C. de Oliveira Filho¹, Carlos A. F. Schettini^{2,*}, Ricardo F. da Silva³, Edmilson S. de Lima⁴, Ernesto de C. Domingues⁵

¹ Programa de Pós-Graduação em Geociências - Universidade Federal de Pernambuco (Av. Prof. Moraes Rego, 1235 - Cidade Universitária, Recife - 50670-901 - PE - Brazil)

² Instituto de Oceanografia - Universidade Federal do Rio Grande (Av. Itália, km 8, Rio Grande - 96000-000 - RS - Brazil)

³ Programa de Pós-Graduação em Geociências - Universidade Federal de Pernambuco (Av. Prof. Moraes Rego, 1235 - Cidade Universitária, Recife - 50670-901 - PE - Brazil)

⁴ Departamento de Geologia - Universidade Federal de Pernambuco (Av. Prof. Moraes Rego, 1235 - Cidade Universitária, Recife - 50670-901 - PE - Brazil)

⁵ Programa de Pós-Graduação em Oceanografia - Universidade Federal de Pernambuco (Av. Prof. Moraes Rego, 1235 - Cidade Universitária, Recife - 50670-901 - PE - Brazil)

* Corresponding author: guto.schettini@gmail.com

ABSTRACT

The Itapessoca estuary is part of the Itamaracá-Itapessoca Estuarine System, a ria-type estuary located on the northeast Brazilian shore, in the state of Pernambuco. Here we present an assessment of the estuarine circulation, suspended sediment dynamics, and its main transport mechanisms. We carried out a field survey where water level, currents, salinity, temperature, and suspended sediment concentration (SSC) were recorded at 10-minute intervals during two complete semi-diurnal tidal cycles under spring tide conditions. The field survey was conducted in September (2012), which is a transitional period between wet and dry seasons. The water level displayed symmetrical ebb-flood phases; however, currents were ebb-dominated. The freshwater contribution was negligible, and the mean salinity was ~35 g/kg, which is slightly lower than the adjacent shelf values (36.5 g/kg). The SSC transport was driven by the ebb-dominated tidal currents, with the highest values of ~30 mg/l occurring during the peak current during the ebb. The source of the suspended sediment was the erosion from the bottom, and the concentration was much lower than other similar estuaries (e.g., Caravelas). This observation suggests this system is a 'sediment starved system' in the sense that it presents a low concentration of suspended sediment.

Descriptors: Estuarine circulation, Tides, Sediment transport.

INTRODUCTION

Estuarine environments play a key role in the mass transfer in the continent-ocean interface (Sweet et al, 1971; Valle-Levinson, 2010). They act as a filter, being efficient traps for sediments and other continent-born materials (Schubel and Kennedy, 1984). The inflow of nutrient-supplied waters makes estuaries highly biological productive environments. Due to their strategic localization, they favor economic

development such as harbor activity, fostering industrial development. This led to some of the largest cities in the world growing on estuarine margins.

The sharp longitudinal gradient of salinity is one of the main characteristics of estuaries. This physical feature produces the longitudinal density gradient which drives the estuarine circulation. A lighter upper layer flows seawards above a denser layer which flows landwards (Cameron & Pritchard, 1963; Geyer & MacCready, 2014). Morphology and winds may also play roles in the circulation, resulting in complex patterns of circulation, mixing, and transport of materials. The several forcings on the hydrodynamics act on broad temporal and spatial scales, which turns the assessment of distribution and transport of

Submitted: 12-Feb-2021

Approved: 07-Aug-2021

Associate Editor: Cesar Rocha



© 2021 The authors. This is an open access article distributed under the terms of the Creative Commons license.

properties into a challenging task (Kjerfve et al., 1982; Valle-Levinson, 2010). These circulation patterns will drive the sediment and other scalar budgets (Dyer, 1995; Uncles, 2002).

There is a rich diversity of estuarine environments along the Brazilian shore, subjected to a variety of physical settings from 33° south to 4° north. In the south, the climate is subtropical and the tidal regime is micro-tidal (D'Aquino et al., 2010). In the north, in contrast, the climate is tropical and the tidal regime is macro-tidal (Asp et al., 2018). Between them, along the Northeast shores, occur patches of tropical and semi-arid climates with tidal regimes ranging from micro to meso-tidal (Schettini et al., 2017; Paiva and Schettini, 2021). The semi-arid climate is severe enough to produce conditions of hypersalinity and inverse estuarine circulation (Schettini et al., 2016; Valle-Levinson and Schettini, 2016). With exception of the São Luis (Maranhão) and Todos os Santos (Bahia) bays, estuaries along this shore are relatively small, making them more prone to human-induced changes (Schettini et al., 2017). Because of the semi-arid climate, most systems present a relatively small freshwater inflow, even with considerably large drainage basins, e.g., the Capibaribe River estuary (Schettini et al., 2017). Some systems present very small drainage basins with the shape of drought river valleys, e.g., the Caravelas estuary (Schettini & Miranda, 2010). These systems may be classified as rias according to the physiographic classification of Fairbridge (1980).

There are two rias in Pernambuco State: the estuary of Formoso River (Silva et al., 2004) and the Itamaracá-Itapessoca Estuarine System (IIES) (Medeiros & Kjerfve, 2005; Schettini et al., 2021). Both are smaller than the Galician rias, known as prototypes of this type of system. Both present relatively small drainage basins and a drought river valley surrounded by relatively high relief. The small drainage basin means reduced freshwater inflow and continent-born sediments. Another feature of these systems is their proportionally larger intertidal areas occupied by mangroves, indicating active sediment trapping (Burchard et al., 2018; Schettini et al., 2020), which seems paradoxical, considering the limited local sediment source. These are tide-dominated systems; taking into account the limited sediment production, it may be possible that a substantial fraction

of the sediments accumulated in the mangroves is imported from the shelf. To improve the understanding of the estuarine dynamics in rias, sediment starved estuaries, we present here an assessment of the circulation and sediment transport in the Itapessoca estuary.

THE STUDY AREA

Itapessoca estuary is a drought river valley unfilled by sediments (e.g., Fairbridge, 1980), interconnected with the Santa Cruz Channel/Itamaracá Island (Medeiros & Kjerfve, 1993 and 2005; Schettini et al., 2021; Oliveira Fo. et al., 2021 - in press) (Figure 1). The system is formed by two channels ~8 km long and 300 m wide, along the flanks of Itapessoca Island. The channels are connected through a narrow and shallow channel in the northern part. The main stream debouching there is Itapessoca Creek, with a drainage basin of 125 km² out of the 1024 km² total watershed area. The land use in the drainage basin is mainly sugar cane crops along with an industrial complex (CPRH, 2003).

The regional climate of the Brazilian Northeast region is semi-arid (Kopen's Aw, tropical savannah). However, along the east shore, a strip (~ 100 km wide) named Zona da Mata (Bush Zone) occurs, where the climate is tropical wet (Kopen's Am, tropical monsoon). The mean annual temperature is 25.5 °C, ranging from 23.9 to 26.6 °C in August and February. In the countryside, the annual precipitation rate is ~600 mm/year, with 5 to 6 dry months. Along the shore, the precipitation rate can exceed 2,000 mm/year, with rains concentrated in the May-July months, although rains occur all year long. In contrast, in the rest of the country, the precipitation is nearly null during the dry months. There are sharp changes in the precipitation regime along the Zona da Mata caused by orography (Pereira, 2013). To characterize the IIES drainage basin climatology, we adopted the values provided by Francisco et al. (2017) for the town of Caaporã, ~20 km north. The mean annual precipitation and evapotranspiration rates are 1,917 and 1,508 mm/year, with a strong seasonal modulation. The rainy period is from May to July, and the dry period is from October to December (Figure 2A).

There is no river flow measurement in the IIES drainage basin, although it has been estimated by Medeiros et al., (1993). Figure 3B shows the monthly climatology of river flow for the Tracunhaém River. This

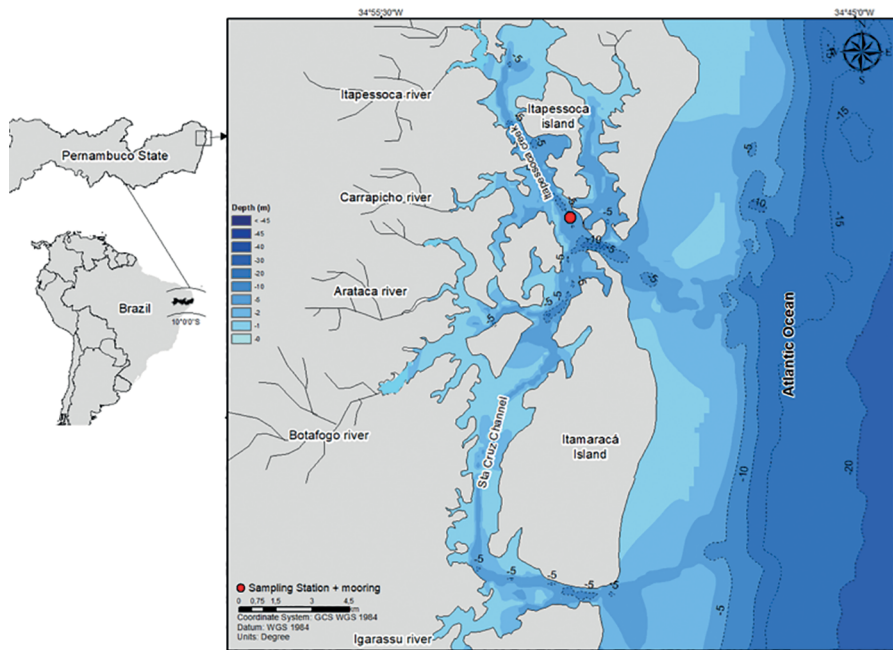


Figure 1. Localization of the Itapessoca Estuary, in the context of South America and Pernambuco State, called the Itamaracá-Itapessoca estuarine system.

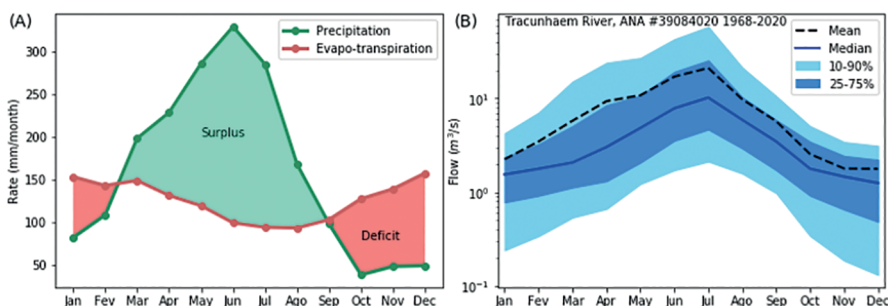


Figure 2. (A) Monthly precipitation and evapo-transpiration rates for Caoporã, a town situated 20 km north of the IIES. (B) Monthly mean and median river flow of the Tracunhaém river, which flows along the western border of the IIES drainage basin.

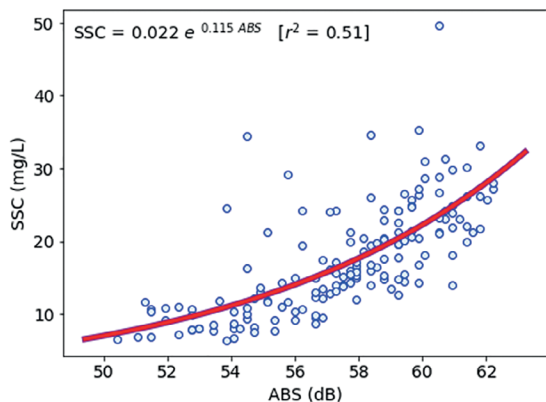


Figure 3. Relationship between the acoustic backscatter (ABS, dB) and suspended sediment concentration (SSC, mg/L) from the moored data.

river borders the western side of the IIES drainage basin (gauged area = 1,230 km²) and reflects the behavior of the IIES streams. The river flow strictly follows the balance between precipitation and evapotranspiration. The maximum monthly mean occurs in July at the end of the rainy period, and the minimum occurs in December at the end of the dry period. The maximum mean value is ~20 m³/s, and the minimum is < 2 m³/s. However, the Tracunhaém drainage basin extends towards the country where the climate changes to semi-arid and a higher flow may be expected towards the coast in proportion to the drainage area. Estimates of the freshwater inflow to the IIES during the dry and wet periods are 0 (null) and ~50 m³/s, respectively (Medeiros and Kjerfve, 1993).

The adjacent inner shelf is narrow (~40 km) with the shelf break at 60–65 m deep (Barcellos et al., 2020). The high salinity (> 36.5 g/kg) and high temperature (> 26 °C) Tropical Water dominates all year long, with little contribution from continental runoff (< 5%) (Domingues et al., 2017). The regional winds are controlled by the South Atlantic High, blowing from the east in summer and from the southeast in winter. Alongshelf currents are driven mainly by northward winds, reversing southwards during summer (Dec/Feb) (Schettini et al., 2017). Regional tides are purely semi-diurnal and range between 0.7 and 2.3 m under neap and spring tide conditions, and explain ~99% of the water level variance at daily time-scales (Schettini et al., 2017).

MATERIAL AND METHODS

FIELD OBSERVATIONS

The field survey was carried out from 28-Sep to 1-Oct, 2012, to gather hydrodynamic and suspended sediment concentration data. An acoustic Doppler current profiler (ADCP), three conductivity-temperature data loggers (CTs), and an optical backscatter turbidity-meter (OBS) were moored at the thalweg of the Itapessoca estuary at 9 m deep and ~0.5 km from the channel mouth (Figure 1). The period of data acquisition comprised two complete semi-diurnal tidal cycles (25 hours).

Water level, current velocity/direction, and acoustic backscatter (ABS) were recorded with an ADCP by Nortek A/S, model Aquadopp Profiler, 1,000 kHz. The ADCP recorded vertical profiles with 0.35 m bin size, with the first bin ~0.9 m above the bottom. Each profile was assembled from an average of 180 s at 2 Hz, at 10-minute intervals. CTs and OBS recorded at 10-minute intervals, performing bursts of 30 s at 1 Hz. The CTs and OBS were by JFE Advantech. The CTs were positioned at the bottom, mid-depth, and at the surface. The OBS was positioned at the bottom. Currents were decomposed to the principal axis component. We use the convention of negative values for the seaward currents and positive values for the landward currents.

SUSPENDED SEDIMENT CONCENTRATION

Suspended sediment concentration (SSC) was derived from the OBS and the acoustic backscatter

(ABS) recorded by the ADCP. Both OBS and ABS are reliable proxies for the estimation of SSC (Schettini et al., 2010). OBS is usually measured in formazin turbidity unit (FTU), and ABS is in decibels (dB). The relationship between OBS and SSC is direct and linear for low SSC conditions (e.g., <500 mg/L, Winterwerp and van Kesteren, 2004). The relationship between ABS and suspended sediment is direct and non-linear (Deines, 1999).

To convert ABS to SSC we adopted the procedure described in Zaleski and Schettini (2006), which is a two-step method. First, we must obtain a relationship between SSC and OBS, as we adapted Equation 1 by Pereira et al., (2010).

$$SSC(OBS) = 1.03 \times OBS - 1.05 \quad (1)$$

with coefficient of determination $r^2 = 0.99$. Although this is a calibration for another estuary, both systems are relatively similar. Both present small drainage basins and are tide-dominated; the SSC is relatively low (<< 1,000 mg/L), draining the same Barreiras geological formation, so we may expect similar sediment characteristics, such as mineralogy assembly and color. Thus, we may use the OBS data recorded at the bottom simultaneously with the ABS to assess the relationship between them.

First, the acoustic intensity recorded by the ADCP in 'counts' must be converted to acoustic power in dB, discounting the basal noise of the instrument, and corrected for the water absorption and conical acoustic beam spreading, using

$$ABS = Kc(E - E_{BN}) + 20 \log_{10}(z) + 2\alpha_w(z) + TS \quad (2)$$

(Deines, 1990; Lohrmann, 2001; Gartner, 2004). The first term on the right side of Equation 2 is the conversion from counts to dB. E is the echo intensity recorded (counts); E_{BN} is the instrument basal noise, or the value of echo intensity recorded when the instrument is in the air; Kc is a factor of conversion from counts to dB. The second term of the right side of Equation 2 accounts for the effect of acoustic spreading along the vertical distance from the instrument. The third term accounts for the acoustic absorption of the water, being the water absorption coefficient which depends on water density. The last term accounts for the suspended acoustic reflectors' target

strength, usually unknown and not considered. The relationship between the SSC and the ABS from the bottom surface cell (0.25 cm from sea level) of the vertical profile is presented in Figure 3. The SSC can be estimated by the ABS by

$$SSC = 0.022e^{0.115ABS} \quad (3)$$

with determination coefficient of $r^2 = 0.51$ (Figure 3). The use of r^2 to quantify the goodness-of-fit for nonlinear models must be used carefully (Spiess and Neymeyer, 2010). Despite the low value (e.g., > 0.7), most of the samples ($N = 158$) are well aligned with the model.

TRANSPORT DECOMPOSITION

The calculation of the mechanisms of advective transport of salt followed the approach described by Miranda et al. (2002), based on Bowden (1963), Fisher (1976), Hunkins (1981), Dyer (1974), and Kjerfve (1986). For a given laterally homogeneous estuarine channel, the decomposition of current u and salinity S are given by

$$\begin{aligned} u(x, z, t) &= u_a(x) + u_t(x, t) + u_s(x, z) + u'(x, z, t) \\ S(x, z, t) &= S_a(x) + S_t(x, t) + S_s(x, z) + S'(x, z, t) \end{aligned} \quad (4)$$

where u_a and u_s are the respective temporal and spatial averaged values, or $\langle \overline{u} \rangle$ and $\langle \overline{S} \rangle$. The overbar denotes vertical averaging, and the brackets denote time averaging. The terms u_t and S_t represent the deviation over time, physically the periodic tidal effects, given by $u_t = \overline{u} - u_a$ and $S_t = \overline{S} - S_a$, and the terms u_s and S_s represent the deviation in space in the water column, physically the stationary tidal effects, given by $u_s = \langle u \rangle - u_a$ and $S_s = \langle S \rangle - S_a$. The last terms, u' and S' , are residuals, which can be attributed to small-scale physical processes, are given by $u' = u - u_a - u_t - u_s$ and $S' = S - S_a - S_t - S_s$.

The water column thickness h also varies with the tide, and can also be decomposed in time as $h(x, t) = h_a + \eta_t(x, t)$, where h_a is the local time averaged water depth $\langle h \rangle$, and η_t is the tidal variation of the water level. The averaged salt transport per one or more tidal cycles T_s is given by

$$T_s = \frac{1}{T} \int_0^T \int_0^h \rho u S dz dt \quad (5)$$

where h is the water column thickness, ρ is the water density, u is the longitudinal component of the current speed, and S is the salinity. The substitution of the different decomposition in the Eq. 4 produces 32 parcels of transport, from which seven have physical significance and are non-zero. The total averaged salt transport per one or more tidal cycles can be written as

$$\begin{aligned} T_s &= \overline{\rho} (u_t h_a S_a + \langle h_t u_t \rangle S_a + h_a \langle u_t S_t \rangle + \\ &iv \quad v \quad vi \quad vii \\ &h_a \overline{u_s S_s} + h_a \langle \overline{u' S'} \rangle + \langle u_t S_t h_t \rangle + u_a \langle S_t h_t \rangle) \end{aligned} \quad (6)$$

where the seven terms inside the parenthesis can be attributed to (i) fluvial discharge or storage term, (ii) Stokes' drift, (iii) tidal velocity-concentration correlation, (iv) gravitational circulation, (v) oscillatory shear, (vi) tidal sloshing, and (vii) tidal concentration-depth correlation (Miranda et al., 2002). The terms from Eq. 5 were divided by the mean depth of the sampling station (~ 7.5 m) to allow comparison with results from Medeiros & Kjerfve (2005). The decomposition applied by these authors is based on Kjerfve (1986), for well-mixed estuaries and did not solve the fourth term of the gravitational mechanism. All the other terms represent the same mechanisms. Equation 6 was applied to 12:20 windows, which take into account 75 temporal samples running over the whole time series. The results were reduced to the mean and standard deviation of each term of the equation.

The transport decomposition can be applied to any scalar property. However, the interpretation of the results must consider if the property is conservative (e.g., salinity) or not (e.g., temperature). In the present case, we applied this to the suspended sediment concentration (e.g., Schettini et al., 2006). The results from the resulting decomposition must be understood as a first approximation of the dominant processes in the site where the data were recorded,

especially when one considers the lateral variability of the flow (McSweeney et al., 2016) and secondary flow (Chant, 2010) in the cross-section, which will affect the distribution of momentum, salinity, and SSC.

RESULTS

The time variation of water level, salinity, the along-estuary component of the velocity, and SSC are presented in Figure 4. The statistics summary is presented in Table 1. The tidal signal displayed a symmetrical pattern, with equivalent periods of flood and ebb. The tidal range was ~2.3 m, which is the regional mean spring tide range. The currents displayed a phase lag, with their peaks occurring at the end of the flood and ebb periods, respectively. The velocity was asymmetric, with maximum ebb velocity (-0.87 m/s) stronger than the maximum flood velocity currents (0.69 m/s).

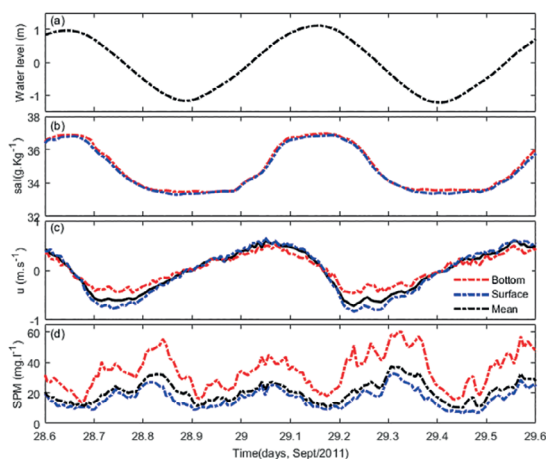


Figure 4. Time series of (a) water level, (b) salinity, (c) longitudinal velocity and (d) suspended sediment concentration.

Table 1. Summary of basic statistics of current velocity, salinity, temperature and SSC.

Parameter	Maximum	Minimum	Mean
U flood (m/s)	0.69		0.36
U ebb (m/s)		-0.87	-0.41
Salinity surface (g/kg)	36.9	33.3	34.8
Salinity bottom (g/kg)	36.9	33.4	34.9
Temperature surface (°C)	27.8	26.7	27.3
Temperature bottom (°C)	27.8	26.8	27.3
SSC (mg/L)	60.0	6.7	20.0

Temporal evolution of salinity followed the water level (Figure 4b), with maximum value (37.0 g/kg) at high tide and minimum value (33.0 g/kg) at low tide, indicating a light degree of dilution by freshwater inflow, although it cannot be defined as hypersaline conditions as previously stated. The salinity at the surface was on average 0.08 g/kg less than the salinity at the bottom, and the highest stratification occurred during low tide. The temperature (not presented in Figure 4) showed a maximum intra-tidal variation of 1 °C, with the highest values of 27.8 °C during the high tides. The SSC ranged between 7 (at the surface) and 60 mg/L (at the bottom), with the highest values during the current velocity peaks and near the bottom.

Figure 5 presents the vertical and temporal distributions of the longitudinal current velocity and SSC with 0.35 m of vertical resolution, which allows a better inspection of the data derived from the ADCP. This figure allows better visualization of the longer flood and shorter ebb current periods. The currents were virtually unidirectional, reversing from ebb to flood vertically monotonic. The SSC presented a quarter-diurnal pattern, with events of higher concentration coinciding with the current velocity peak. During the periods of slack waters, at high and low tide, the vertical SSC decreased in the whole water column.

The relationship between the current velocity and the water level, the tidal stage diagram, is presented in Figure 6. The evolution of the tide condition presented an upside-down raindrop shape, near-circular, which indicates a standing wave regime when there is no mass transport by wave movement.

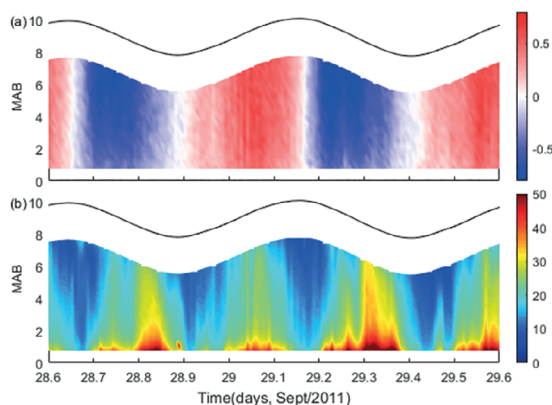


Figure 5. Temporal and vertical variation of (a) longitudinal velocity (m/s) and (b) SSC (mg/L). MAB means meters above the bed.

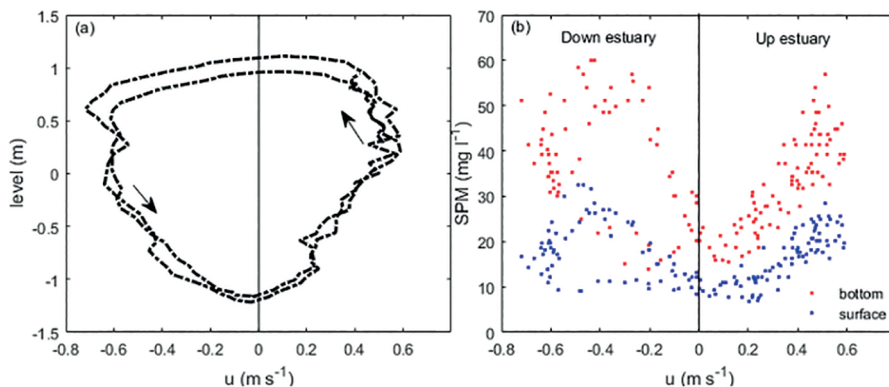


Figure 6. (a) the tide stage diagram, relating the variation of the velocity and water level, and (b) the relationship between current velocity and SSC at the surface and at the bottom.

The current velocity asymmetry is indicated by the displacement for the negative (ebb) values. The relationship between current velocity and SSC presents an asymmetric butterfly shape, with an indication of hysteresis during the ebb period (i.e., the water tending to maintain the same asymmetric shape).

The results from the decomposition of the transport of suspended sediments are presented in Table 2 and Figure 7. The total transport was -2.12 kg/m.s , with the negative sign indicating seawards. The dominant mechanisms were the mean transport and the tidal correlation, with similar values and seawards. The other relevant mechanisms were the Stokes drift, gravitational circulation, and tidal shear, all with about the same magnitude and landwards. All mechanisms displayed a temporal variability; however, this was clearer for the largest ones, semi-diurnal.

Table 2. Mechanisms of the advective transport of suspended sediments calculated by Equation 6.

Terms	Transport (kg/s.m)
i (mean transport)	-2.17 ± 0.78
ii (Stokes drift)	0.44 ± 0.06
iii (tidal correlation)	-2.69 ± 1.47
iv (gravitational circulation)	0.33 ± 0.04
v (tidal pumping)	0.03 ± 0.00
vi (tidal shear)	0.40 ± 0.04
vii (low frequency fluctuations)	0.01 ± 0.00
Sum of terms above	-3.64 ± 2.17
Total	-3.57 ± 2.10

DISCUSSION

Along the shores of Pernambuco occur several coastal embayments. We can separate them into two groups: those with larger drainage basins, and others with reduced drainage basins. The former still have relatively small drainages, not exceeding $10,000 \text{ km}^2$ (e.g., Capibaribe and Una Rivers). Further, as they are subjected to a semi-arid climate in the countryside, their water production is below the average for systems with equivalent sizes. During the dry period, their flow rate is low and they will work as efficient traps, retaining sediments and other river-borne materials such as pollutants. The occurrence of estuarine turbidity maxima in these systems is a strong indicator of that (Schettini et al., 2016; Arruda-Santos et al., 2018).

During the wet period, extreme precipitation events occur (Ratisbona, 1976), and can produce

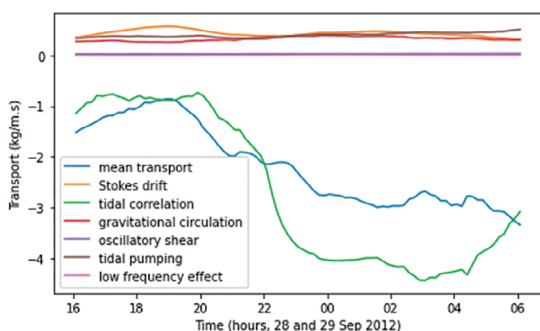


Figure 7. Temporal variation of each right-side term of Equation 6, listed in the color indication legend.

massive injections of materials to the coastal zone. A single extreme event can produce more material transport than the expected volume during years under average conditions (Schettini, 2002). Once on the shelf, these materials will be dispersed according to the shelf currents and waves. During the wet period, the currents are predominately northwards (Schettini et al., 2017; Domingues et al., 2017), and this could allow these materials to be exchanged with other estuaries by tidal action (Wolanski et al., 1992; Schettini et al., 2013). The IIES is a short distance from the highly polluted Capibaribe estuary (Oliveira et al., 2014; Régis et al., 2018), which is a pollutant source for the coastal area (Maciel et al., 2016). So, despite the IIES being relatively depopulated and preserved, it may be trapping materials delivered by the Capibaribe estuary.

Our survey provided a snapshot of the circulation and sediment dynamics, capturing the spring tidal regime, during the transition period between wet and rainy periods. The freshwater content can be easily assessed using the salinity. Regional continental shelf salinity is ~ 36.5 g/kg (Schettini et al., 2017), and the average salinity at the monitored station was ~ 35 g/kg, which disregarding other more complicated factors controlling the salinity distribution (Dyer, 1997), indicates that 96% of the water volume moving back and forth forced by the tides is marine. Further, we can scale the relative importance of the freshwater inflow by the flow ratio: the ratio between the freshwater volume contributions during $\frac{1}{2}$ tidal periods to the tidal prism volume. The tidal prism can be scaled by the product between the system area and the tidal range (Kjerfve, 1990). The West channel of Itapessoca Island has an area of ~ 20 km², and with a tidal range of 2.3 m, the tidal prism is $\sim 46 \times 10^6$ m³. There is no river discharge data available, but we may guess a value of about 1.5 m³/s based on Medeiros and Kjerfve (1996). The resulting flow ratio is $\sim 7 \times 10^{-4}$. It indicates that the water exchange with the adjacent shelf contributes 1000 times more than the local river inflow. Thus, we can hypothesize that all other properties measured at that point are driven mostly by tides, with negligible freshwater or river-borne materials content. The sediments are river-borne, but then are reworked materials from past freshet events. Their source could be either the local drainage or the exchange with the shelf.

The presence of suspended sediments in the water is a matter of energy/turbulence to keep the high-density particles suspended in a less dense environment and material availability. Turbulence is produced by vertical shear caused by the bottom drag, produced either by currents or waves. Long-period wave energy (generated offshore) is mostly dumped in the inlets. Short-period waves (generated locally) can be considered to have a minor role because of the limited fetch, as the system is mostly geographically orientated orthogonal to the prevailing wind regime. So, most of the water-bed momentum exchanged is due to the tidal currents, which is higher during the peak currents during flood and ebb. The highest SSC was recorded during these moments (Figure 5 and 6b), indicating that the main source of the material is the resuspension from the bed instead of horizontal advection (e.g., Schettini et al., 2013). This is corroborated by the relationship between the depth-averaged SSC and the bottom SSC (Figure 8) (e.g., Nichols, 1984; Siegle et al. 2009), which can be used as an indicator of the suspended sediment source. A good agreement (higher r^2) suggests the bottom as the main source, meanwhile, a poor agreement indicates other sources.

The Caravelas Estuary (Bahia, Brazil) is relatively similar to the Itapessoca system. They share a similar climate, similar tidal regimes and present common physiographic features, such as small drainage basins and multiple inlet systems. There are more assessments on the Caravelas Estuary dynamics (Schettini and Miranda, 2010; Pereira et al., 2010; Schettini et al., 2013; Andutta et al., 2013; Sousa et al., 2014). However, an important distinction is the adjacent shelf characteristics. The shelf off

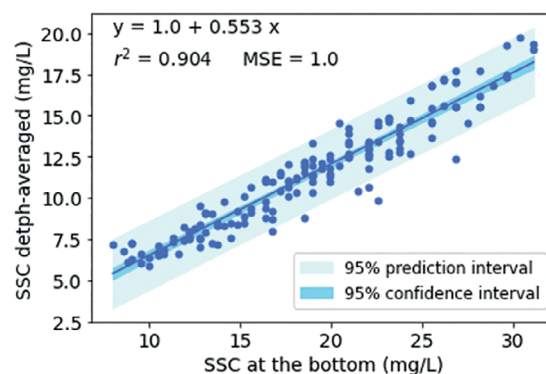


Figure 8. Relationship between depth-averaged SSC and bottom SSC. MSE: mean squared error.

Caravelas is wider due to the presence of Abrolhos Bank, with large carbonate reefs affecting the coastal dynamics and allowing mud accumulation on the inner shelf. The shelf off IIES is narrow and dominated by sand and carbonate biogenic sandy-gravel, poorly sorted sediments with low organic matter contents of natural marine origin (Barcellos et al., 2020 ; Oliveira Filho et al., 2021 (in press)). The fine sediment availability is lower, and this is reflected in the levels of SSC. In Caravelas, the SSC can be >300 mg/L during the spring tides (Schettini et al., 2013), while in Itapessoca the highest SSC was ~30 mg/L. This is particularly puzzling when one considers the extensive areas of mangroves in the system. This suggests that the systems may be a 'sediment starved system' which depends on the allochthonous sources (e.g., Willemsen et al., 2016), a concern in face of the sea level rise.

CONCLUSIONS

In this study, we assessed the circulation and dynamics of suspended sediments in the western channel of the Itapessoca Island. It is part of the Itamaracá-Itapessoca Estuarine System. The assessment was based on a field survey that captures two complete tidal cycles, at spring tide. Our results showed that the hydrodynamics were primarily ruled by the tides, with negligible effects from freshwater inflow. Currents were ebb-dominant, as well as the residual suspended sediment transport. The source of suspended sediment was erosion from the bottom, and the concentration was much lower than other similar estuaries. From our findings, we suggest this is a 'sediment starved system', which is particularly sensitive to sea-level rise.

AUTHOR CONTRIBUTIONS

J.C.O.F: Investigation, formal analysis, visualization and writing original draft;

C.A.F.S: Conceptualization, investigation, fund acquisition, methodology, formal analysis, writing review-editing;

R.F.S: Investigation, writing-review editing;

E.S.L: Conceptualization, investigation, writing-review and editing;

E.C.D: Investigation, methodology

ACKNOWLEDGEMENTS

We thank Pernambuco State Science Foundation (FACEPE) for providing the means to perform the field activity by funding the project MuGloEst

(APQ-0079-1.08/11). Thanks to Prof. Juan F. Paniagua-Arroyave and the other anonymous reviewers for their suggestions for the manuscript.

REFERENCES

- ANDUTTA, F. P., MIRANDA, L. B., SCHETTINI, C. A. F., SIEGLE, E., SILVA, M. P., IZUMI, M. V. & CHAGAS, F. M. 2013. Temporal variations of temperature, salinity and circulation in the Peruípe river estuary (Nova Viçosa, BA). *Continental Shelf Research*, 11(70), 36-45.
- ARRUDA-SANTOS, R. H., SCHETTINI, C. A. F., YOGUI, G. T., MACIEL, D. C. & ZANARDI-LAMARDO, E. 2018. Sources and distribution of aromatic hydrocarbons in a tropical marine protected area estuary under influence of sugarcane cultivations. *Science of Total Environment*, 624, 935-944.
- ASP, N. E., GOMES, V. J. C., SCHETTINI, C. A. F., SOUZA-FILHO, P. W. M., SIEGLE, E., OGSTON, A. S., NITTRouer, C. A., SILVA, J. N. S., NASCIMENTO JUNIOR, W. R., SOUZA, S. R., PEREIRA, L. C. C. & QUEIROZ, M. C. 2018. Sediment dynamics of a tropical tide-dominated estuary: turbidity maximum, mangroves and the role of the Amazon River sediment load. *Estuarine, Coastal and Shelf Science*, 214, 10-24.
- BARCELLOS, R. L., MELO, M. C. S. S., SIAL, A. N. & MANSO, V. A. V. 2020. Sedimentary organic matter characterization on a tropical continental shelf in Northeastern Brazil. *International Journal of Geosciences*, 11(6), 393-419.
- BOWDEN, K. F. 1963. The mixing processes in a tidal estuary. *Journal of Air and Water Pollution*, 7, 343-356.
- BURCHARD, H., SCHUTTELAARS, H. M. & RALSTON, D. K. 2008. Sediment trapping in estuaries. *Annual Review of Marine Science*, 10, 371-395.
- CAMERON, W. N. & PRITCHARD, E. 1963. Estuaries. In: HILL, M. N. (ed.). *The sea*. New York: John Wiley & Sons, pp. 306-324.
- CHANT, R. J. 2010. Estuarine secondary circulation. In: VALLE-LEVINSON, A. (ed.). *Contemporary issues in estuarine physics*. Cambridge: Cambridge University Press, pp. 100-124.
- CPRH (Companhia Pernambucana do Meio Ambiente). 1998. *Diagnóstico sócio ambiental e mapeamento das potencialidades e restrições de uso: área piloto da RBMA – Complexo de Igarassu, Itapissuma e Itamaracá*. Recife: CPRH.
- CPRH (Companhia Pernambucana do Meio Ambiente). Agência Estadual do Meio Ambiente de Pernambuco. 2003. *Diagnóstico socioambiental do litoral norte de Pernambuco*. Recife: CPRH.
- D'AQUINO, C. A., NETO, J. S. A., MANIQUE, G. A. B. & SCHETTINI, C. A. F. 2011. Caracterização oceanográfica e do transporte de sedimentos em suspensão no estuário do Rio Mampituba, SC. *Revista Brasileira de Geofísica*, 29(2), 217-230.
- D'AQUINO, C. A., PEREIRA FILHO, J. & SCHETTINI, C. A. F. 2010. Fluvial modulation of hydrodynamics and salt transport in a highly stratified estuary. *Brazilian Journal of Oceanography*, 58(2), 165-175.
- DEINES, K. L. 1999. Backscatter estimation using broadband acoustic Doppler current profilers. In: *Proceedings of the IEEE Sixth Working conference on Current Measurements*, San Diego, California, 13-16 September 1999. San Diego: IEEE, pp. 249-253.
- DYER, K. R. 1974. The salt balance in stratified estuaries. *Estuarine and Coastal Marine Science*, 2(3), 273-281.

- DYER, K. R. & NEW, A. L. 1986. Intermittency in estuarine mixing. In: WOLFE, D. A. (ed.). *Estuarine variability*. Orlando: Academic Press, pp. 321-339.
- DYER, K. R. 1988. Fine sediment particle transport in estuaries. In: DRONKERS, J. & VAN LEUSSEN, W. (eds.). *Hydrodynamic of estuaries*. New York: Springer, pp. 295-310.
- DYER, K. R. 1998. *Estuaries: a physical introduction*. 2nd ed. Chichester: John Wiley & Sons.
- FAIRBRIDGE, R. W. 1980. The estuary: its definition and geodynamic cycle. In: OLAUSSON, E. & CATO, I. (eds.). *Chemistry and biogeochemistry of estuaries*. New York: John Wiley & Sons, pp. 1-35.
- FIDEM (Fundação de Desenvolvimento da Região Metropolitana do Recife). 1987. *Série Desenvolvimento Urbano e Meio Ambiente. Proteção de áreas estuarinas de Pernambuco*. Recife: FIDEM.
- FISCHER, H. B. 1976. Mixing and dispersion in estuaries. *Annual Review of Fluid Mechanics*, 8, 107-133.
- GARTNER, J. W. 2004. Estimating suspended solid concentrations from backscatter intensity measured by Doppler current profiler in San Francisco Bay, California. *Marine Geology*, 211(3-4), 169-187.
- GEYER, W. R., BEARDSLEY, R. C., LENTZ, E. J., CANDELA, J., LIMBURNER, R., JOHNS, W. E., CASTRO, B. M. & SOARES, I. D. 1996. Physical oceanography of the Amazon shelf. *Continental Shelf Research*, 16(5-4), 575-616, DOI: [https://doi.org/10.1016/0278-4343\(95\)00051-8](https://doi.org/10.1016/0278-4343(95)00051-8)
- GEYER, W. R. & KINEKE, G. C. 1995. Observations of currents and water properties in the Amazon frontal zone. *Journal of Geophysical Research: Oceans*, 100(C2), 2321-2339, DOI: <https://doi.org/10.1029/94JC02657>
- GEYER, W. R. & MACREADY, P. 2014. The estuarine circulation. *Annual Review of Fluid Mechanics*, 46, 175-197.
- HANSEN, D. V. & RATTRAY JUNIOR, M. 1965. Gravitational circulation in straits and estuaries. *Journal of Marine Research*, 23(2), 104-122.
- HANSEN, D. V. & RATTRAY JUNIOR, M. 1966. New dimension in estuary classification. *Limnology and Oceanography*, 11(3), 319-325.
- HUNKINS, K. 1981. Salt dispersion in the Hudson estuary. *Journal of Physical Oceanography*, 11, 729-738.
- JAY, D. A. & MUSIAK, J. D. 1994. Particle trapping in estuarine tidal flows. *Journal of Geophysical Research*, 99(C10), 20445-20461.
- KJERFVE, B. 1986. Circulation and salt flux in a well mixed estuary. In: VAN DE KREEKE, J. (ed.). *Physics of shallow estuaries and bays*. New York: Springer-Verlag, pp. 22-29.
- KJERFVE, B. 1990. *Manual for investigation of hydrological processes in Mangrove Ecosystems*. New Delhi: UNESCO/UNDP.
- KJERFVE, B., PROEHL, J. A., SCHWING, F. B., SEIM, H. E. & MAROZAS, M. 1982. Temporal and spatial considerations in measuring estuarine water fluxes. In: KREEKE, V. S. (ed.). *Estuarine comparisons*. New York: Academic Press, pp. 37-51.
- LESSA, G. C., DOMINGUEZ, J. M. L., BITTENCOURT, A. C. S. P. & BRICHTA, A. 2001. The tides and tidal circulation of Todos os Santos Bay, Northeast Brazil. *Anais da Academia Brasileira de Ciências*, 73(2), 245-261, DOI: <http://dx.doi.org/10.1590/S0001-37652001000200009>
- LOHRMANN, A. 2001. *Monitoring sediment concentration with acoustic backscattering instruments*. Norway: Nortek AS, Nortek Technical Note N. 03.
- MACIEL, D. C., SOUZA, J. R. B., TANIGUCHI, S., BICEGO, M. C., SCHETTINI, C. A. F. & ZANARDI-LAMARDO, E. 2016. Hydrocarbons in sediments along a tropical estuary-shelf transition area: sources and spatial distribution. *Marine Pollution Bulletin*, 113(1-2), 566-571, DOI: <http://dx.doi.org/10.1016/j.marpolbul.2016.08.048>
- MCDUGALL, T. J. & BARKER, P. M. 2011. Getting started with TEOS-10 and the Gibbs Seawater (GSW) oceanographic toolbox [online]. Arnhem: SCOR/IAPSO WG127/UNESCO. Available at: http://www.teos-10.org/pubs/Getting_Started.pdf [Accessed: 15, Jul. 2015].
- MCSWEENEY, J. M., CHANT, R. J. & SOMMERFIELD, C. K. 2016. Lateral variability of sediment transport in the Delaware estuary. *Journal of Geophysical Research: Oceans*, 121(1), 725-744, DOI: <https://doi.org/10.1002/2015JC010974>
- MEDEIROS, C. 1991. *Physical characteristics and circulation-dispersion processes in the Itamaraca estuarine system, Brazil*. PhD. Columbia: University of South Carolina, Marine Science Program.
- MEDEIROS, C. & KJERFVE, B. 1993. Hydrology of a tropical estuarine system: Itamaraca, Brazil. *Estuarine, Coastal and Shelf Science*, 36, 495-515.
- MEDEIROS, C. & KJERFVE, B. 2005. Longitudinal salt and sediment fluxes in a tropical estuary: Itamaraca, Brazil. *Journal of Coastal Research*, 21(4), 751-758.
- MIRANDA, L. B., CASTRO, B. M. & KJERFVE, B. 2002. *Princípios de oceanografia física de estuários*. São Paulo: EDUSP (Editora da Universidade de São Paulo).
- NICHOLS, M. M. 1984. Effects of fine sediment resuspension in estuaries. In: MEHTA, A. J. (ed.). *Estuarine cohesive sediment dynamics*. Berlin: Springer-Verlag, pp. 5-42.
- OFFICER, C. B. 1976. *Physical oceanography of estuaries and associated coastal waters*. New York: John Wiley & Sons.
- OFFICER, C. B. 1977. Longitudinal circulation and mixing relations in estuaries. In: OFFICER, C. B. (ed.). *Estuaries, geophysics, and the environment*. Washington: National Academy of Sciences, pp. 13-21.
- OLIVEIRA FILHO, J. C., SOTTOLICCHIO, A., HUYBRECHTS, N. & SCHETTINI, C. A. F. in press. Residual circulation in a semi-enclosed tropical embayment with complex geometry. *Regional Studies in Marine Science*.
- OLIVEIRA, T. S., BARCELLOS, R. L., SCHETTINI, C. A. F. & CAMARGO, P. B. 2014. Processo sedimentar atual e distribuição da matéria orgânica em um complexo estuarino tropical, Recife, PE, Brasil. *Journal of Integrated Coastal Zone Management*, 14(3), 399-411.
- PAIVA, B. P. & SCHETTINI, C. A. F. 2021. Circulation and transport processes in a tidally forced salt-wedge estuary: the São Francisco river estuary, Northeast Brazil. *Regional Studies in Marine Science*, 41, 101602.
- PEREIRA, M. D., SIEGLE, E., MIRANDA, L. B. & SCHETTINI, C. A. F. 2010. Hidrodinâmica e transporte de material particulado em suspensão sazonal em um estuário dominado por maré: Estuário de Caravelas (BA). *Revista Brasileira de Geofísica*, 28(3), 427-444.

- PRANDLE, D. 2009. Estuaries: dynamics, mixing, sedimentation and morphology. Cambridge: Cambridge University Press.
- PRITCHARD, D. W. 1955. Estuarine circulation patterns. *Proceedings of the American Society of Civil Engineers*, 81, 1-11.
- PRITCHARD, D.W. 1989. Estuarine classification — a help or a hindrance. In: NEILSON, B. J., KUO, A. & BRUBAKER, J. (eds.). *Estuarine circulation. contemporary issues in science and society*. New Jersey: Humana Press, pp. 1-38.
- RATISBONA, L. R. 1976. The climate of Brazil. In: SCHWERDTFGER, W. (ed.). *Climates of South and Central America*. Amsterdam: Elsevier, pp. 219-93.
- RÉGIS, C. G., SOUZA-SANTOS, L. P., YOGUI, G. T., MORAES, A. S. & SCHETTINI, C. A. F. 2018. Use of Tisbe biminiensis nauplii in ecotoxicological tests and geochemical analyses to assess the sediment quality of a tropical urban estuary in northeastern Brazil. *Marine Pollution Bulletin*, 137, 45-55.
- SCHETTINI, C. A. F. 1994. *Determinantes hidrológicas na manutenção da hipersalinidade da lagoa de Araruama, RJ*. MSc. Niterói: UFF (Universidade Federal Fluminense).
- SCHETTINI, C. A. F. 2002. Near bed sediment transport in the Itajaí-Açu River estuary, southern Brazil. In: WINTERWERP, J. C. & KRANENBURG, C. (eds.). *Fine sediment dynamics in the marine environment*. New York: Elsevier, pp. 499-512.
- SCHETTINI, C. A. F., ALMEIDA, D. C., SIEGLE, E. & ALENCAR, A. C. B. 2010. A snapshot of suspended sediments and fluid mud distributions in the Tijucas Bay (Brazil): a mixed-energy environment. *Geo-Marine Letters*, 30(1), 47-62.
- SCHETTINI, C. A. F., ASP, N. E., OGSTON, A. S., GOMES, V. J. C., MCLACHLAN, R. L., FERNANDES, M. E. B., NITTRouer, C. A., TRUCOLO, E. C. & GARDUNHO, D. C. L. 2020. Circulation and fine-sediment dynamics in the Amazon Macrotidal Mangrove Coast. *Earth Surface Processes and Landforms*, 45(3), 574-589, DOI: <https://doi.org/10.1002/esp.4756>
- SCHETTINI, C. A. F. & CARVALHO, J. L. B. 1999. Caracterização hidrodinâmica do estuário do rio Cubatão, Joinville. *Nota técnicas FACIMAR*, 3, 87-97.
- SCHETTINI, C. A. F. & MIRANDA, L. B. 2010. Circulation and suspended sediment particulate matter transport in a tidally dominated Estuary: Caravelas Estuary, Bahia, Brazil. *Brazilian Journal of Oceanography*, 58(1), 1-11.
- SCHETTINI, C. A. F., MIRANDA, J. B., VALLE-LEVINSON, A. & TRUCOLO, E. C. 2016. The circulation of the lower Capibaribe estuary (Brazil) and its implications for the transport of scalars. *Brazilian Journal of Oceanography*, 64(3), 263-276.
- SCHETTINI, C. A. F., PEREIRA, M. D., SIEGLE, E., MIRANDA, L. B. & SILVA, M. P. 2013. Residual fluxes of suspended sediment in a tidally dominated tropical estuary. *Continental Shelf Research*, 70, 27-35.
- SCHETTINI, C. A. F., RICKLEFS, K., TRUCOLO, E. C. & GOLBIG, V. 2006. Synoptic hydrograph of a highly stratified estuary. *Ocean Dynamics*, 56(3-4), 308-319.
- SCHETTINI, C. A. F., SILVA, L. A., VALENÇA, L. M. M. & MANSO, V. A. V. 2021. Transport processes in the Santa Cruz Channel, Brazil. *Regional Studies in Marine Science*, 45, 101812, DOI: <https://doi.org/10.1016/j.rsma.2021.101812>
- SCHETTINI, C. A. F., VALLE-LEVINSON, A. & TRUCOLO, E. C. 2017. Circulation and transport in short, low-inflow estuaries under anthropogenic stresses. *Regional Studies in Marine Science*, 10, 52-64.
- SCHUBEL, J. R. & KENNEDY, V. S. 1984. The estuary as a filter: an introduction. In: KENNEDY, V. S. (ed.). *The estuary as a filter*. Cambridge: Academic Press, pp. 1-11, DOI: <https://doi.org/10.1016/B978-0-12-405070-9.50007-4>
- SIEGLE, E., SCHETTINI, C. A. F., KLEIN, A. H. F. & TOLDO JUNIOR, E. E. 2009. Hydrodynamics and suspended sediment transport in the Camboiú Estuary Brazil: pre-jetty condition. *Brazilian Journal of Oceanography*, 57(2), 123-135.
- SILVA, M. H., PASSAVANTE, J. Z. O., SILVA-CUNHA, M. G. G., VIEIRA, D. A. N., GREGO, C. K. S. & MUNIZ, K. 2004. Distribuição espacial e sazonal da biomassa fitoplanctônica e dos parâmetros hidrológicos no estuário do rio Formoso (Rio formoso, Pernambuco, Brasil). *Tropical Oceanography*, 32(1), 89-106.
- SOUSA, S. H. M., AMARAL, P. G. C., MARTINS, V., FIGUEIRA, R. C. L., SIEGLE, E., FERREIRA, P. A. L., SILVA, I. S., SHINAGAWA, E., SALAROLI, A., SCHETTINI, C. A. F., SANTA-CRUZ, J. & MAHIQUES, M. M. 2014. Environmental evolution of the Caravelas Estuary (Northeastern Brazilian coast, 17°S, 39°W) based on multiple proxies in a sedimentary record of the last century. *Journal of Coastal Research*, 30(3), 474-486.
- SPIESS, A. N. & NEUMEYER, N. 2010. An evaluation of R2 as an inadequate measure for nonlinear models in pharmacological and biochemical research: a Monte Carlo approach. *BMC Pharmacology*, 10, 6, DOI: <https://doi.org/10.1186/1471-2210-10-6>
- SRH-PE (Secretaria de Recursos Hídricos do Estado de Pernambuco). 2010. *Plano hidroambiental da bacia hidrográfica do Rio Capibaribe: Tomo I - diagnóstico hidroambiental*. Recife: SRH-PE - Projetos Técnicos.
- SWEET, D. C. 1971. *The economic and social importance of estuaries*. Washington: Environmental Protection Agency, Water Quality Office, Technical Support Division.
- UNCLES, R. J. 2002. Estuarine physical processes research: some recent studies and progress. *Estuarine Coastal and Shelf Science*, 55(6), 829-856.
- VALLE-LEVINSON, A. 2010. Definition and classification of estuaries. In: VALLE-LEVINSON, A. (ed.). *Contemporary issues in estuarine physics*. Cambridge: Cambridge University Press, pp. 1-11.
- VALLE-LEVINSON, A. & SCHETTINI, C. A. F. 2016. Fortnightly switching of residual flow drivers in a tropical semiarid estuary. *Estuarine Coastal and Shelf Science*, 169, 46-55.
- WILLEMSEN, P. W. J. M., HORSTMAN, E. M., BORSJE, B. W., FRIESS, D. A. & DOHMEN-JANSSEN, C. M. 2016. Sensitivity of the sediment trapping capacity of an estuarine mangrove forest. *Geomorphology*, 273, 189-201.
- WINTERWERP, J. C. & VAN KESTEREN, W. G. M. 2004. *Introduction to the physics of cohesive sediment dynamics in the marine environment*. New York: Elsevier.
- WOLANSKI, E., MAZDA, Y. & RIDD, P. 1992. Mangrove hydrodynamics. In: ROBERTSON, A. I. & ALONGI, D. M. (eds.). *Tropical mangrove ecosystems*. Washington: American Geophysical Union, pp. 436-462, DOI: <https://doi.org/10.1029/CE041p0043>
- ZALESKI, A. R. & SCHETTINI, C. A. F. 2006. Procedimentos para calibração de perfiladores acústicos de corrente por efeito doppler para a determinação da concentração de material particulado em suspensão na água. *Revista Brasileira de Recursos Hídricos*, 11(3), 191-200.